Significant coercivity enhancement at low temperatures in magnetically oriented cobalt ferrite nanoparticles

Pablo Tancredi[a,b]*, Patricia C. Rivas-Rojas[b,c], Oscar Moscoso-Londoño[d], Diego Muraca[e], Marcelo Knobel[e], Leandro M. Socolovsky[f]

[a] *Functional Nanomaterials – INTI-Micro and Nanotechnology, National Institute of Industrial Technology, San Martín, Buenos Aires, CP B1650, Argentina*

[b] *Laboratory of Amorphous Solids – INTECIN, Faculty of Engineering, University of Buenos Aires – CONICET, Buenos Aires, CP C1063, Argentina*

[c] *Laboratory of Applied Crystallography, School of Science and Technology, National University of San Martin, San Martin, Buenos Aires, CP B1650, Argentina.*

[d] *Autonomous University of Manizales, Antigua Estación del Ferrocarril, Manizales, CP 170001, Colombia*

[e] *Instituto de Física "Gleb Wataghin", University of Campinas (UNICAMP), Campinas, SP, CEP 13083-859, Brazil*

[f] *Santa Cruz Regional School, National Technological University - CIT Santa Cruz (CONICET), Río Gallegos, Santa Cruz, CP Z9400, Argentina*

ABSTRACT

The present work describes a synthesis and characterization strategy employed to study the magnetic anisotropic properties of a diluted nanoparticulated system. The system under analysis is composed of monodisperse and highly-crystalline 16 nm $Co_{0.5}Fe_{2.5}O_4$ nanoparticles, homogenously dispersed in 1-octadecene. Owing to the liquid nature of the matrix at room temperature, the relative orientation of the nanoparticles easy axis can be controlled by an external magnetic field, enabling us to measure how the magnetic properties are modified by the alignment of the particles within the sample. In turn, by employing this strategy we have found a significant hardness and squareness enhancement of the hysteresis loop in the magnetically oriented system, with the coercive field reaching a value as high as 30.2 kOe at low temperatures. In addition, the magnetic behavior associated with the system under study was supported by additional magnetic measurements, which were ascribed to different events expected to take place throughout the sample characterization, such as the melting process of the 1-octadecene matrix or the NPs relaxation under the Brownian mechanism at high temperatures.

* Corresponding Author: Pablo Tancredi (ptancredi@fi.uba.ar)

The magnetic behavior of a nanoparticulated system is defined by its intrinsic structural properties, which can be classified and studied in different and correlated complexity levels. One of these levels is defined by the inherent characteristics of the nanoparticles (NPs), and can be associated with features such as the NPs composition, degree of crystallinity, size and shape. Among the different types of magnetic NPs, Co-based ferrites ($Co_xFe_{3-x}O_{4-\delta}$) stand out as a very interesting and popular system, with appealing properties and a broad range of technological applications. In recent years, many studies have been devoted to understand how the magnetic behavior of these type of nanostructures are defined by the aforementioned features, granting a general and fair consensus about the relationships between these two topics[1–7].

A second level is related to the magnetic interparticle interactions, mostly those of the dipolar type. Magnetic interactions play an important role in nanostructured systems, and are fundamental to fully understand the behavior of rather concentrated and granular systems, in which the ideal, non-interacting superparamagnetic model is not sufficient to describe the experimental observations[8–10].

Last, a third level can be associated with the relative orientation and relaxation mechanisms of the NPs. The dependence between the magnetic properties, the easy axis orientation and the direction of the external magnetic field has been a topic of moderate research, addressed by theoretical studies[11–13] and some experimental reports in thin films and magnetic fluids[14–16]. Owing to their high magneto crystalline anisotropy, Co-based ferrite NPs can be an attractive material to study how these structural features define the macroscopic behavior of a specific nanoparticulated system.

The orientation of the NPs easy axis can be achieved by applying a DC magnetic field during an immobilization process, like the curing of a polymer. This kind of strategy has been used to study the alignment of $L1_0$-FePt NPs[17] and commercial Fe_3O_4 NPs[18,19]. A different immobilization approach relies in the freezing process of a carrier solvent, a strategy that has been employed in the study of highly monodisperse Fe_3O_4 NPs[16,20]. In the latter cases, the immobilization of the NPs and the orientation dependence of the magnetic properties were found to be a very useful tool to analyze and discuss the relaxation mechanisms behind the sample's magnetization dynamics.

In the case of Co-based ferrite NPs, the relative orientation phenomenon has been used to explain certain differences observed in the magnetic behavior of NPs with equal composition and primary size[21]. Nevertheless, specific and systematic studies addressing this approach from an experimental perspective are still missing.

Taking into account the research background presented above, we decided to design a characterization strategy that allowed us to manipulate the relative orientation of a set of Co-based ferrite NPs immersed in an insulating matrix, and subsequently measure how the magnetic properties are modified by the alignment of the particles within the sample, especially at low temperatures.

A sample of Co-based ferrite NPs (CoFe oxide NPs) was synthesized by thermal decomposition employing a hot-injection approach. Initially, a Co and Fe oleate precursor was prepared with $FeCl_3 \cdot 6H_2O$ (Anedra, reagent grade) and $CoCl_2 \cdot 6H_2O$ (Laboratorios Cicarelli, reagent grade) by a ligand exchange process as reported in the literature[22], and dissolved in 1-octadecene (Aldrich, 90%) to a final concentration of 0.5 M. To carry out the NPs formation reaction, 2.5 ml of 1-octadecene and 2.5 ml of oleic acid (Aldrich, 90%) were mixed in a flask and heated to 315 °C. Then, 4 ml of the Co and Fe oleate solution was slowly added over the next 180 min (addition rate approx. 22.2 µl/min) and heated for another 30 min. The mixture was cooled to room temperature and the NPs were precipitated by the addition of ethanol. After several washing steps, the NPs were mixed with toluene to produce a stable suspension. The described hot-injection strategy is based on the "Extended Lamer" synthesis approach recently reported by Vreeland *et al.*[23]. This approach has proven to be an excellent alternative to prepare high-quality nano monocrystals, with the ability to precisely tune the size and composition of the NPs.

Fig. 1(a) shows an image of the synthesized oleic acid-capped CoFe oxide NPs, acquired with a JEOL TEM-FEG (JEM 2100F) Transmission Electron Microscope. The NPs are fairly spherical and present a rather narrow polydispersity, with a mean diameter of 16 ± 3 nm. The X-Ray diffractogram measured on the dry NPs powder presented in Fig. 1(b) reveals that the cubic spinel-type structure associated with a Co-based ferrite phase (JCPDS card No. 22-1086) is the only contribution present in the sample. No trace of rock salt metal oxides (such as FeO or CoO) was detected, so the occurrence of exchange-bias can be discarded. The crystallite size calculated by the Scherrer equation was about 13 nm, slightly below the mean diameter obtained by TEM. A dark field HR-TEM image of a single particle is presented in Fig. 1(c) and confirms the monocrystalline nature of the NPs, as suggested by the Scherrer equation. The elemental composition was measured by Energy

Dispersive X-ray Spectroscopy. The Co-to-Fe ratio was found to be approximately 1-to-5, resulting in a system with a chemical formula of $Co_{0.5}Fe_{2.5}O_4$. The hydrodynamic diameter measured in toluene by Dynamic Light Scattering was about 20 nm, and verifies that the formation of agglomerates is avoided and the NPs are individually stabilized in the solvent.

In order to study the dependence of the magnetic properties at low temperature with the nano-crystal relative orientation, a strategy was designed to let the NPs rotate under an applied magnetic field. At first, 10 drops of 1-octadecene were added to 1 ml of the CoFe oxide NPs toluene dispersion. 1-octadecene is a long chain alkene with a melting point around 288 K. The toluene was evaporated from the mixture and the oily matrix with the homogenously dispersed CoFe oxide NPs was introduced in the SQUID chamber (Quantum Design MPMS XL-5 SQUID magnetometer). The NPs volume fraction in the sample is approximately 0.2 %, meaning that the system is highly diluted and the magnetic dipolar interactions between NPs can be negligible.

At 300 K 1-octadecene is in liquid state, so the CoFe oxide NPs can freely rotate in the medium and orientate their magnetic easy-axis with an external magnetic field. Also, the liquid matrix will allow the NPs to relax under the Brownian mechanism. When cooling the sample below the 1-octadecene melting point, the CoFe oxide NPs will freeze in their current position and no further physical rotation will be possible. If no magnetic field is applied while cooling below 288 K, the NPs will freeze with their magnetic moments in random orientations. On the other hand, if a strong magnetic field is present, the NPs will freeze in magnetically oriented positions. Unlike other orientation strategies reported in the literature, this freezing process is expected to be reversible, due to the possibility of re-melting the 1-octadecene and letting the NPs freely rotate by the Brownian relaxation mechanism above 288 K. In addition, because the orientation process is carried out inside the SQUID chamber by the homogenous magnetic field provided by the SQUID magnetometer, a uniform alignment of the NPs without significant gradients of concentration is also expected. A scheme describing this strategy is shown in Fig. 2.

Fig. 3(a) and 3(b) present the Magnetization vs. Applied Field (M vs. H) hysteresis loops at 5 K and 300 K, respectively. According to the proposed measurement strategy, the Zero Field Cooling (ZFC) protocol should led to a randomly oriented NPs system (RO-CoFe NPs). The coercive field (H_C) at 5 K in RO-CoFe NPs was found to be about 21.1 kOe, a standard and frequently reported value in the literature for highly-crystalline and spherical $Co_xFe_{3-x}O_{4-\delta}$ NPs prepared by thermal decomposition[1,24–26]. The strong anisotropy associated with this high H_C can be related to the presence of Co^{2+} ions on the octahedral B sites of the spinel structure[5,27]. Also, higher H_C values are expected for NPs with spherical shapes due to the increase of the surface anisotropy[2]. The Saturation Magnetization (M_S) was found to be around 95 emu/g, which is also consistent with previous results on similar NPs[24,28,29]. The reduced remnant magnetization (M_R/M_S) in this sample is about 0.86, a value that is a fingerprint of a system with cubic anisotropy[30]. This result suggests that the magnetic behavior of the NPs is governed by the cubic symmetry of the magnetocrystalline anisotropy of $Co_xFe_{3-x}O_{4-\delta}$, at least at low temperatures.

In a system with cubic anisotropy and randomly oriented magnetic moments, a first and rough approximation of the effective anisotropy constant (K_{eff}) at low temperatures can be calculated by $K_{eff} = \rho H_K M_S/0.64$, with ρ being the Co ferrite density and H_K the anisotropy field. By assuming that H_C at 5 K is a good estimation of H_K, the calculated K_{eff} is 1.7×10^7 erg/cm^3, which is consistent with previous literature reports on similar systems and comparable to the bulk magnetocrystalline anisotropy (1.9×10^7 erg/cm^3)[1,29,31]. Recent reports have shown that the magnetic anisotropy of spherical, highly-crystalline CoFe oxide NPs larger than 10 nm can change upon varying the temperature[3,29]. In this case, the variation of the NPs anisotropy is suggested by the evolution of M_R/M_S. As showed in Fig. 3(c), this value shifts from 0.86 at 5 K to 0.5 at 250 K, meaning that the anisotropy may change from cubic to uniaxial as the temperature increases.

The magnetic orientation of the CoFe oxide NPs was achieved by applying a Field Cooling (FC) protocol (H = 60 kOe). The M vs. H curve of the magnetically oriented NPs system (MO-CoFe NPs) presents a significant enhancement of the hysteresis loop hardness and squareness, reflected in a noticeable increase of both H_C and remanence (M_R). At this measurement condition, the saturation of the sample was not fully reached even for fields up to 60 kOe. Nevertheless, the estimated H_C was found to be about 30.2 kOe, which represents a nearly 45% increase with respect to the RO-CoFe NPs. Similarly, M_R also displays a significant enhancement, from 0.86 to 0.94 (expressed as M_R/M_S). These values are among the highest H_C and M_R reported to date for a set of Co-based ferrite NPs, even exceeding by a wide margin other previous records measured at low temperatures[1,31]. Under this characterization strategy, the critical modification of the hysteresis loop can be easily

related to the alignment of the highly anisotropic Co-based ferrite NPs. The hardness and squareness increase are also evident when calculating the $(BH)_{MAX}$ product. In turn, this value changes from 7.4 MGOe in RO-CoFe NPs to 8.8 MGOe in MO-CoFe NPs.

Two types of sample arrangements were measured at 300 K. The *M* vs. *H* curve of CoFe oxide NPs dispersed in 1-octadecene shows a practically negligible coercive field. At 300 K, the NPs in the liquid matrix are free to shift the alignment of their magnetic moment due to physical rotation (Brownian reversion mechanism), leading to a magnetic behavior that can be assimilable to a superparamagnetic system. The asymmetry and open segments observed in the hysteresis loop can be associated with the presence of a very small fraction of fixed NPs unable to physically rotate despite the melted matrix[22]. A second sample was measured as a dry and solid CoFe oxide NPs powder, so the possibility of physical rotation is revoked. The *M* vs. *H* curve of this arrangement presents a H_C of 0.68 kOe, evidencing that the fixed NPs are still at the blocked regime at 300 K. This result is consistent with previous literature reports that present H_C values around 0.5 to 1.0 kOe for Co-based ferrite NPs between 15 to 20 nm[1,7,32,33].

Fig. 4(a) shows the Magnetization vs. Temperature (*M* vs. *T*) curves measured following the ZFC-FC protocol. The ZFC curves of the CoFe oxide NPs dispersed in 1-octadecene present a clear and sharp peak between 285 and 300 K. Despite some similarities with the commonly reported unblocking events of magnetic NPs, the sharp peak observed in this system is directly related to the melting process of the 1-octadecene, which enables the physical rotation and the alignment of the formerly fixed CoFe oxide NPs with the external magnetic field. The position of the maximum was found to be independent from the applied field, proving that this event is strictly related to a structural evolution of the material (melting process of the matrix) instead of the unblocking event of the magnetic NPs due to Néel relaxation. ZFC curves with similar sharp peaks have been previously reported for other systems undergoing the melting process of the matrix, for both iron oxide and Co-based ferrite NPs[34,35]. The melting of the matrix is also responsible of the peaks evidenced in the FC curves. In this case, the increase of the applied field during the cooling process seems to attenuate the sharpness of the peak. This result is consistent with the idea that the orientation degree of the NPs is defined by the intensity of the applied field of the FC protocol. In this sense, if a system with a significant fraction of magnetically oriented NPs is heated from low temperatures, the initial magnetization will be relatively high and there will be no chance to undergo a second orientation process during the matrix melting event, thus leading to an attenuated increase of the magnetization during this transition.

Finally, the ZFC *M* vs. *T* curve of the dry and solid CoFe oxide NPs powder was found to have a mild and monotonic increase, as shown in Fig. 4(b). The absence of any defined peak in this measurement suggests that the blocking temperature of the fixed NPs is above 300 K, an expected result according to the size and composition of the studied nanostructure.

In summary, we have presented a synthesis and characterization strategy that allowed us to manipulate the relative orientation of a set of magnetic NPs and measure how the magnetic properties at low temperatures are modified by the alignment of the particles within the sample. We have tested this strategy on a sample composed of 16 nm highly crystalline oleate-capped $Co_{0.5}Fe_{2.5}O_4$ NPs and we have found a significant hardness and squareness enhancement of the hysteresis loop at 5 K when comparing the results of the magnetically oriented with the randomly oriented system. In the magnetically oriented system, we measured a coercive field of 30.2 kOe and a remanence magnetization of 0.94, which are the highest values reported to date for a set of Co-based ferrite NPs at low temperatures. We have performed other support magnetic measurements, and ascribe the observed behavior to different events expected to take place throughout the sample characterization, such as the melting process of the 1-octadecene matrix or the NPs relaxation under the Brownian mechanism.

In the near future, we hope this characterization strategy may become a useful alternative for the nano-magnetism community to explore the magnetic and anisotropic properties of cobalt and iron oxide NPs prepared by thermal decomposition approaches.

ACKOWNLEDGEMENTS

P.T., P.C.R.-R., and L.M.S. acknowledge Argentinean agency CONICET for financial support. D. M. and M.K. acknowledges the National Council for Scientific and Technological Development (CNPq) grant #425501/2018-3, Brazilian agencies Fundação de Amparo à Pesquisa do Estado de São Paulo (FAPESP), grant #17/10581, Brazilian Nanotechnology National Laboratory (LNNano) for the use of electron microscopy facility, project number ME-22345.

REFERENCES

[1] H. Sharifi Dehsari and K. Asadi, J. Phys. Chem. C **122**, 29106 (2018).
[2] Q. Song and Z.J. Zhang, J. Am. Chem. Soc. **126**, 6164 (2004).
[3] T.E. Torres, E. Lima, A. Mayoral, A. Ibarra, C. Marquina, M.R. Ibarra, and G.F. Goya, J. Appl. Phys. **118**, (2015).
[4] L.T. Lu, N.T. Dung, L.D. Tung, C.T. Thanh, O.K. Quy, N. V. Chuc, S. Maenosono, and N.T.K. Thanh, Nanoscale **7**, 19596 (2015).
[5] A. Franco and F.C. E Silva, Appl. Phys. Lett. **96**, 2010 (2010).
[6] E. Fantechi, G. Campo, D. Carta, A. Corrias, C. De Julián Fernández, D. Gatteschi, C. Innocenti, F. Pineider, F. Rugi, and C. Sangregorio, J. Phys. Chem. C **116**, 8261 (2012).
[7] A. Sathya, P. Guardia, R. Brescia, N. Silvestri, G. Pugliese, S. Nitti, L. Manna, and T. Pellegrino, Chem. Mater. **28**, 1769 (2016).
[8] O. Moscoso-Londoño, D. Muraca, K.R. Pirota, M. Knobel, P. Tancredi, L.M. Socolovsky, P. Mendoza Zélis, D. Coral, M.B. Fernández van Raap, U. Wolff, V. Neu, C. Damm, and C.L.P. de Oliveira, J. Magn. Magn. Mater. **428**, 105 (2017).
[9] P.C.R. Rojas, P. Tancredi, O.M. Londoño, M. Knobel, and L.M. Socolovsky, J. Magn. Magn. Mater. **451**, 688 (2018).
[10] D. Peddis, F. Orrù, A. Ardu, C. Cannas, A. Musinu, and G. Piccaluga, Chem. Mater. **24**, 1062 (2012).
[11] J. García-Otero, A.J. García-Bastida, and J. Rivas, J. Magn. Magn. Mater. **189**, 377 (1998).
[12] J.C. Eloi, M. Okuda, S. Correia Carreira, W. Schwarzacher, M.J. Correia, and W. Figueiredo, J. Phys. Condens. Matter **26**, (2014).
[13] I. Conde-Leborán, D. Serantes, and D. Baldomir, J. Magn. Magn. Mater. **380**, 321 (2015).
[14] F. Ilievski, A. Cuchillo, W. Nunes, M. Knobel, C.A. Ross, and P. Vargas, Appl. Phys. Lett. **95**, 0 (2009).
[15] M. Klokkenburg, B.H. Erné, V. Mendelev, and A.O. Ivanov, J. Phys. Condens. Matter **20**, (2008).
[16] M. Klokkenburg, B.H. Erné, and A.P. Philipse, Langmuir **21**, 1187 (2005).
[17] Y. Tamada, S. Yamamoto, S. Nasu, and T. Ono, Phys. Rev. B - Condens. Matter Mater. Phys. **78**, 1 (2008).
[18] G. Shi, R. Takeda, S.B. Trisnanto, T. Yamada, S. Ota, and Y. Takemura, J. Magn. Magn. Mater. **473**, 148 (2019).
[19] T. Yoshida, Y. Matsugi, N. Tsujimura, T. Sasayama, K. Enpuku, T. Viereck, M. Schilling, and F. Ludwig, J. Magn. Magn. Mater. **427**, 162 (2017).
[20] S.A. Shah, D.B. Reeves, R.M. Ferguson, J.B. Weaver, and K.M. Krishnan, Phys. Rev. B - Condens. Matter Mater. Phys. **92**, 1 (2015).
[21] D. Peddis, C. Cannas, A. Musinu, A. Ardu, F. Orruì, D. Fiorani, S. Laureti, D. Rinaldi, G. Muscas, G. Concas, and G. Piccaluga, Chem. Mater. **25**, 2005 (2013).
[22] A.P. Herrera, C. Barrera, Y. Zayas, and C. Rinaldi, J. Colloid Interface Sci. **342**, 540 (2010).
[23] E.C. Vreeland, J. Watt, G.B. Schober, B.G. Hance, M.J. Austin, A.D. Price, B.D. Fellows, T.C. Monson, N.S. Hudak, L. Maldonado-Camargo, A.C. Bohorquez, C. Rinaldi, and D.L. Huber, Chem. Mater. **27**, 6059 (2015).
[24] G. Lavorato, M. Alzamora, C. Contreras, G. Burlandy, F.J. Litterst, and E. Baggio-Saitovitch, Part. Part. Syst. Charact. **36**, 1 (2019).
[25] B. Aslibeiki, P. Kameli, H. Salamati, G. Concas, M. Salvador Fernandez, A. Talone, G. Muscas, and D. Peddis, Beilstein J. Nanotechnol. **10**, 856 (2019).
[26] K. Gandha, K. Elkins, N. Poudyal, and J. Ping Liu, J. Appl. Phys. **117**, 2 (2015).
[27] Y. Melikhov, J.E. Snyder, D.C. Jiles, A.P. Ring, J.A. Paulsen, C.C.H. Lo, and K.W. Dennis, J. Appl. Phys. **99**, (2006).
[28] D. Li, H. Yun, B.T. Diroll, V.V.T. Doan-Nguyen, J.M. Kikkawa, and C.B. Murray, Chem. Mater. **28**, 480 (2016).
[29] A. López-Ortega, E. Lottini, C.D.J. Fernández, and C. Sangregorio, Chem. Mater. **27**, 4048 (2015).
[30] N.A. Usov and S.E. Peschany, J. Magn. Magn. Mater. **174**, 247 (1997).
[31] S.T. Xu, Y.Q. Ma, G.H. Zheng, and Z.X. Dai, Nanoscale **7**, 6520 (2015).
[32] Y. Kumar, A. Sharma, M.A. Ahmed, S.S. Mali, C.K. Hong, and P.M. Shirage, New J. Chem. **42**, 15793 (2018).
[33] L. Wu, P.-O. Jubert, D. Berman, W. Imaino, A. Nelson, H. Zhu, S. Zhang, and S. Sun, Nano Lett. **14**, 3395 (2014).
[34] P. De La Presa, Y. Luengo, V. Velasco, M.P. Morales, M. Iglesias, S. Veintemillas-Verdaguer, P. Crespo, and A. Hernando, J. Phys. Chem. C **119**, 11022 (2015).
[35] R. Di Corato, A. Espinosa, L. Lartigue, M. Tharaud, S. Chat, T. Pellegrino, C. Ménager, F. Gazeau, and C. Wilhelm, Biomaterials **35**, 6400 (2014).

Fig. 1. (a) TEM image of CoFe oxide NPs. (b) X-Ray diffraction pattern of CoFe oxide NPs. (c) Dark-Field HR-TEM image of a highly-crystalline single-phase CoFe oxide NP.

Fig. 2. Schematic illustration showing the two freezing possibilities. The black arrows inside the NPs stand for the magnetization easy axis.

Fig. 3. (a) *M* vs. *H* hysteresis loops at 5 K of RO-CoFe NPs and MO-CoFe NPs. (b) *M* vs. *H* hysteresis loops at 300 K of CoFe oxide NPs in 1-octadecene and as dry powder. Inset: zoom at low fields. (c) H_C and M_R/M_S vs. *T* of RO-CoFe NPs. Table: Parameters extracted from the *M* vs. *H* hysteresis loops at 5 K.

Fig. 4. (a) *M* vs. *T* curves measured following the ZFC (black) and FC (red) protocols of CoFe oxide NPs in 1-octdecene. (b) *M* vs. *T* curve measured following the ZFC protocol of CoFe oxide NPs as dry powder.

PLEASE CITE THIS ARTICLE AS DOI: 10.1063/1.5131259

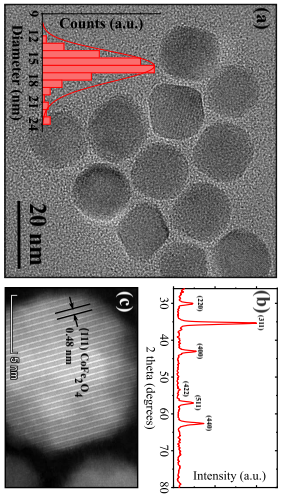

PLEASE CITE THIS ARTICLE AS DOI: 10.1063/1.5131259

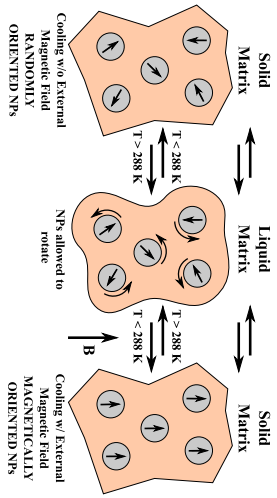

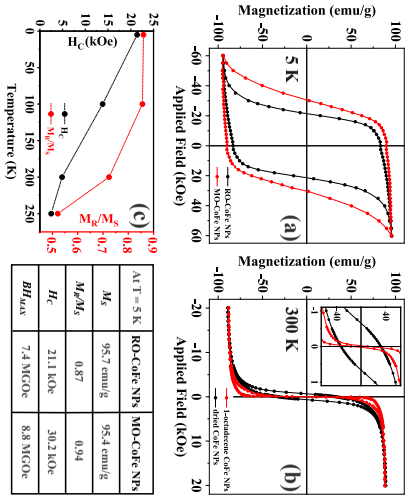

At T = 5 K	RO-CoFe NPs	MO-CoFe NPs
M_S	95.7 emu/g	95.4 emu/g
M_R/M_S	0.87	0.94
H_C	21.1 kOe	30.2 kOe
BH_{MAX}	7.4 MGOe	8.8 MGOe

PLEASE CITE THIS ARTICLE AS DOI: 10.1063/1.5131259